


УДК 546.571+546.18+546.28+546.221+544.344

Slyvka A.A., PhD student.  0000-0002-9173-731X;Bilanych V.S., C.Sc., Assoc. Prof., Head of the Department of Applied Physics and Quantum Electronics.  0000-0003-4293-5675.

IONIC TRANSPORT AND MECHANICAL PROPERTIES OF $\text{Ag}_{7-x}(\text{Ge}_{1-x}\text{P}_x)\text{S}_5\text{I}$ SUPERIONIC CERAMICS

*Uzhhorod National University, Pidgirna St. 46, 88000, Uzhhorod; Ukraine**e-mail: vitaliy.bilanych@uzhnu.edu.ua*

The ionic transport and mechanical properties of $\text{Ag}_{7-x}(\text{Ge}_{1-x}\text{P}_x)\text{S}_5\text{I}$ superionic ceramics and $\text{Ag}|\text{Ag}_{7-x}(\text{Ge}_{1-x}\text{P}_x)\text{S}_5|\text{Se}$ heterostructures were investigated. Charge–discharge processes were studied using cyclic potentiostatic chronoamperometry, while current–voltage characteristics were measured by cyclic voltammetry. The obtained $I(t)$ dependences exhibit a pronounced relaxation behavior and are well described by a two-exponential model, indicating the coexistence of fast interfacial and slow diffusion-controlled processes. The current–voltage characteristics demonstrate nonlinearity, hysteresis, and current maxima associated with interfacial polarization, space-charge formation, and Ag_2Se layer formation at the $\text{SE}|\text{Se}$ interface. It was established that repeated cycling leads to stabilization of the interfacial region and a decrease in nonequilibrium processes. Mechanical properties were studied by micro- and nanoindentation methods. The results revealed a correlation between hardness, elastic modulus, structural disorder, and Ag^+ ionic mobility. A decrease in mechanical rigidity was accompanied by enhanced ionic transport, indicating the important role of structural “softness” in superionic conductivity.

Keywords: superionic ceramics, ionic transport, $\text{Ag}_{7-x}(\text{Ge}_{1-x}\text{P}_x)\text{S}_5\text{I}$, charge–discharge processes, cyclic voltammetry, chronoamperometry, nanoindentation, structural disorder, solid-state electrolytes.

Introduction

Lithium-free superionic materials based on argyrodite compounds $\text{Ag}_{7-x}(\text{Ge}_{1-x}\text{P}_x)\text{S}_5\text{I}$ attract considerable interest for modern solid-state energy applications due to their high ionic conductivity, chemical stability, and potential use in safe next-generation electrochemical devices [1–4]. In the context of the rapid development of solid-state batteries, memristive structures, and electrochemical sensors, particular attention is focused on materials capable of providing efficient ion transport in the solid phase while maintaining sufficient mechanical stability [5–7].

The high ionic conductivity of argyrodite superionic materials is determined by the особенностями their crystal structure, which is characterized by a partially disordered silver sublattice and the presence of a system of energetically close positions for Ag^+ ion hopping [2, 3, 8]. In such compounds, a three-dimensional network of diffusion channels is formed, ensuring high mobility of silver ions and low activation energies for ion migration [3,9]. One of the most

effective approaches for controlling transport properties is heterovalent substitution $\text{Ge}^{4+} \leftrightarrow \text{P}^{5+}$, which leads to changes in vacancy concentration, the degree of structural disorder, and the topology of Ag^+ migration pathways [8–11]. As a result, not only the electrical parameters but also the mechanical properties of the material are modified.

Despite significant progress in the study of ionic transport in superionic materials, the relationship between transport and mechanical characteristics remains insufficiently investigated [6,10,12]. For solid-state electrochemical systems, mechanical stability plays a fundamentally important role because ion migration, space-charge accumulation, and interfacial interaction processes are accompanied by local deformations, variations in internal stresses, and structural rearrangement of the material [5,13]. Of particular importance is the investigation of the correlation between nanomechanical parameters – hardness, elastic modulus, and local deformability – and the kinetics of charge–discharge processes.

In heterostructures of the $\text{Ag|Ag}_{7-x}(\text{Ge}_{1-x}\text{P}_x)\text{S}_5\text{I|Se}$ type, charge transport processes are determined not only by bulk diffusion of Ag^+ ions in the superionic electrolyte but also by interfacial reactions at the solid electrolyte/selenium cathode interface [13-15]. During charging, Ag^+ ions migrate toward the SE|Se interface, followed by the formation of an Ag_2Se phase possessing mixed ionic-electronic conductivity [14, 15]. The charge and discharge processes are accompanied by space-charge accumulation, interfacial polarization, and relaxation phenomena, which strongly depend on the structure and mechanical state of the material [13, 16].

The mechanical properties of the material become one of the factors affecting the efficiency and stability of electrochemical processes. Investigation of the correlation between mechanical properties and charge–discharge processes in $\text{Ag}_{7-x}(\text{Ge}_{1-x}\text{P}_x)\text{S}_5\text{I}$ superionic ceramics is an important task from both fundamental and applied perspectives. Establishing the relationship between structural disorder, mechanical “softness” of the material, and the kinetics of Ag^+ transport makes it possible to gain a deeper understanding of the physical mechanisms governing the operation of solid-state electrochemical systems and to determine approaches for optimizing materials for solid-state energy devices.

The aim of this work is to investigate the ionic transport properties of $\text{Ag|Ag}_{7-x}(\text{Ge}_{1-x}\text{P}_x)\text{S}_5\text{I|Se}$ heterostructures based on the analysis of charge–discharge processes, relaxation characteristics, and the mechanical properties of $\text{Ag}_{7-x}(\text{Ge}_{1-x}\text{P}_x)\text{S}_5\text{I}$ superionic ceramics.

Materials and Methods

Lithium-free superionic ceramic materials of the $\text{Ag}_{7-x}(\text{Ge}_{1-x}\text{P}_x)\text{S}_5\text{I}$ system with different Ge/P ratios were investigated. Based on these materials, solid-state heterostructures of the $\text{Ag|Ag}_{7-x}(\text{Ge}_{1-x}\text{P}_x)\text{S}_5\text{I|Se}$ type were fabricated [17]. Ceramic disks with a diameter of about 10 mm and a thickness of ~1 mm were used as solid electrolytes. A selenium film with a thickness of ~8 μm was deposited on one side of the sample by thermal evaporation in vacuum, followed by the formation of a thin gold current-collecting contact on top of the selenium layer (Fig. 1a). Silver electrodes were then applied to both sides of the disks. As a result, an electrochemical cell

Ag|SE|Se was formed, where SE denotes the $\text{Ag}_{7-x}(\text{Ge}_{1-x}\text{P}_x)\text{S}_5\text{I}$ superionic electrolyte (Fig. 1b). The silver electrode at the Ag|SE interface served as a source of Ag^+ ions [17, 18].

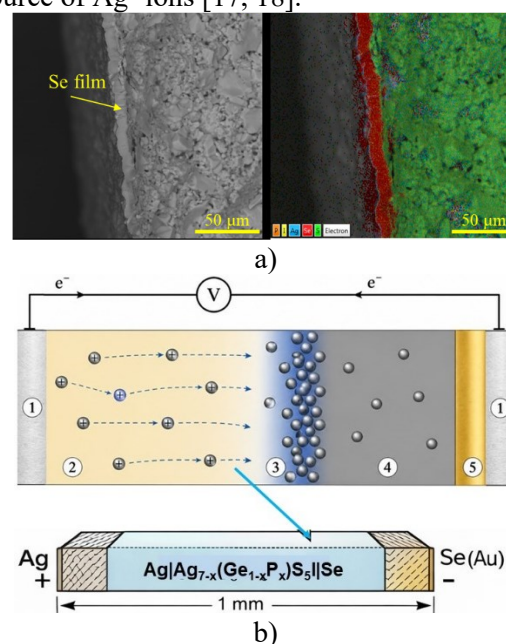


Fig. 1. Structure of the Ag|SE|Se electrochemical cell based on $\text{Ag}_{7-x}(\text{Ge}_{1-x}\text{P}_x)\text{S}_5\text{I}$ superionic ceramics: (a) SEM image of a “fresh” fracture of the SE|Se heterostructure; (b) design of the electrochemical cell and the physical mechanism of charge–discharge processes. 1 – silver electrode, 2 – SE, 3 – interfacial region, 4 – selenium cathode, 5 – gold film.

The ionic transport processes were studied using cyclic potentiostatic chronoamperometry and cyclic voltammetry methods [18,19]. Measurements were performed using an Autolab PGSTAT302F potentiostat/galvanostat. To investigate the current–time dependences $I(t)$, a voltage of $U = 0.4 \text{ V}$ was applied to the electrochemical cell for 600 s (charging mode), after which the voltage was reduced to $U = 0 \text{ V}$ for 600 s (discharging mode). The measurements were carried out in a cyclic regime (5 consecutive cycles) at a temperature of 20 °C. The current–voltage characteristics (CVCs) were measured by cyclic voltammetry under linear voltage sweep conditions [20].

Nanomechanical properties were investigated by instrumental micro- and nanoindentation methods. Mechanical characteristics were determined and analyzed from load–displacement curves (“P–h” diagrams, where P is the indenter load and h is the

indentation depth) using the Oliver–Pharr method [21]. Hardness H was determined from the indentation depth, while the Young's modulus E was calculated from the initial linear part of the unloading branch of the P – h diagram.

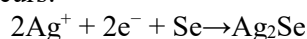
Operating Principle of the $\text{Ag}|\text{Ag}_{7-x}(\text{Ge}_{1-x}\text{P}_x)\text{S}_5\text{I}|\text{Se}$ Electrochemical Cell

In these electrochemical cells, processes of ionic conduction and reversible electrochemical reactions occur at the interfaces. The silver electrode (Ag) serves as a source of the ion-mobile Ag^+ component. The $\text{Ag}_{7-x}(\text{Ge}_{1-x}\text{P}_x)\text{S}_5\text{I}$ solid electrolyte exhibits superionic conductivity due to the high mobility of silver ions within the crystal lattice. Its function in the cell is to provide Ag^+ transport from the silver electrode to the opposite electrode. The selenium electrode (Se) acts as a cathode material in which silver ion intercalation processes can occur with the formation of Ag_2Se -type compounds.

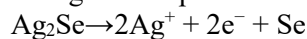
During charging of the electrochemical cell, a positive external potential is applied to the silver electrode. Under its action, silver atoms are oxidized according to the reaction:



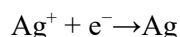
Ag^+ ions migrate through the $\text{Ag}_{7-x}(\text{Ge}_{1-x}\text{P}_x)\text{S}_5\text{I}$ superionic electrolyte toward the Se cathode. At the $\text{SE}|\text{Se}$ interface, the reduction reaction occurs:



As a result, Ag_2Se crystallites are formed at the $\text{SE}|\text{Se}$ interface and within the volume of the selenium film [22]. During discharge, when the polarity of the external voltage is reversed, the reverse reaction becomes thermodynamically favorable. The Ag_2Se compound decomposes:



Ag^+ ions return to the solid electrolyte and diffuse toward the silver electrode, where they are reduced:



Silver is deposited again on the anode, while the selenium-based electrode is released from the inserted ions. Thus, a fully solid-state mechanism is realized in the cell, in which Ag^+ ions migrate through the solid electrolyte, whereas electrons are transported through the external circuit. The key reversible process determining the charge–discharge characteristics is the formation and decomposition of Ag_2Se at the $\text{SE}|\text{Se}$ interface.

Charge–Discharge Processes in $\text{Ag}|\text{Ag}_{7-x}(\text{Ge}_{1-x}\text{P}_x)\text{S}_5\text{I}|\text{Se}$ Heterostructures

Charge accumulation and relaxation processes in solid-state electrochemical cells $\text{Ag}|\text{Ag}_{7-x}(\text{Ge}_{1-x}\text{P}_x)\text{S}_5\text{I}|\text{Se}$ were investigated by cyclic potentiostatic chronoamperometry. A voltage of $U=0.4$ V was applied to the cell for 600 s (charging mode), after which the voltage was reduced to $U=0$ V for 600 s (discharging mode). The measurements were performed in a cyclic regime over 5 cycles at a temperature of 20 °C. The current–time dependences $I(t)$, reflecting the kinetics of Ag^+ ion transport, space-charge accumulation, and interfacial polarization processes, were recorded. Figure 2 shows the charge–discharge current–time dependences for five cycles of the $\text{Ag}|\text{Ag}_{6.5}\text{P}_{0.5}\text{Ge}_{0.5}\text{S}_5\text{I}|\text{Se}$ cell. The $I(t)$ dependences for cells with other compositions exhibit qualitatively similar behavior. The obtained $I(t)$ dependences demonstrate a pronounced relaxation character. At the moment when the voltage is applied, a sharp current jump is observed due to the rapid transport of Ag^+ ions and charging of the electrical double layer at the electrode|electrolyte interfaces. Subsequently, the current monotonically decreases with time, which is associated with system relaxation, redistribution of silver ions, and polarization accumulation in the $\text{SE}|\text{Se}$ interfacial region. Upon switching to the discharge mode, the current changes sign and also exhibits a relaxation decay behavior.

Analysis of the $I(t)$ dependences showed that they can be adequately described by a two-exponential function (Fig. 3):

$$I(t) = I_0 + A_1 e^{-\frac{t}{\tau_1}} + A_2 e^{-\frac{t}{\tau_2}}$$

where I_0 is the asymptotic current value at $t \rightarrow \infty$; A_1 , A_2 are the amplitudes of the corresponding relaxation processes; and τ_1 and τ_2 are the characteristic relaxation times.

The use of a two-exponential approximation indicates the presence of at least two physical mechanisms of charge transport. The fast component with relaxation time τ_1 corresponds to interfacial processes, including charging of the electrical double layer, Ag^+ ion transport in the near-surface region, and the initial stages of Ag_2Se interfacial layer formation. The slow component τ_2 is associated with bulk diffusion of Ag^+ ions in the superionic electrolyte,

relaxation of the space charge, and further development of the SE|Se interfacial region.

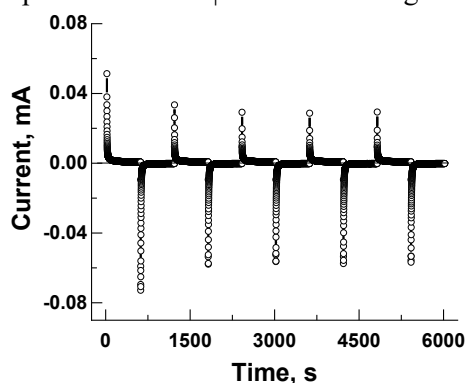


Fig. 2. Current–time dependences of the charging currents (upper part) and discharging currents (lower part) for the $\text{Ag}_{6.5}\text{P}_{0.5}\text{Ge}_{0.5}\text{S}_5\text{I}$ composition at a temperature of $20\text{ }^\circ\text{C}$ and a charging voltage of 0.4 V .

For the $\text{Ag}_{6.5}\text{P}_{0.5}\text{Ge}_{0.5}\text{S}_5\text{I}$ composition at a temperature of $20\text{ }^\circ\text{C}$, the characteristic relaxation times were $\tau_1 \approx 1.4\text{ s}$ and $\tau_2 \approx 40.1\text{ s}$ for the charging process, and $\tau_1 \approx 5.6\text{ s}$ and $\tau_2 \approx 29.3\text{ s}$ for the discharging process.

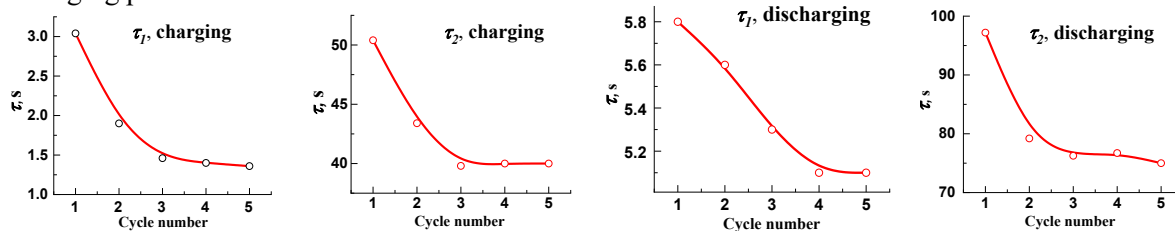


Fig. 4. Changes in the relaxation times τ_1 and τ_2 during five charging and discharging cycles of the $\text{Ag}|\text{Ag}_{6.5}(\text{Ge}_{0.5}\text{P}_{0.5})\text{S}_5\text{I}|\text{Se}$ heterostructure at a temperature of $20\text{ }^\circ\text{C}$.

The relaxation times change with increasing charge–discharge cycle number: from cycle to cycle, they exhibit a tendency toward stabilization (Fig. 4). The most significant changes are observed between the first and subsequent cycles. The first cycle corresponds to the stage of heterostructure and SE|Se interfacial region formation, redistribution of Ag^+ ions, and establishment of an efficient electrical contact. In subsequent cycles, the system reaches a quasi-stationary state characterized by more reproducible $I(t)$ dependences.

The numerical values of τ_1 and τ_2 differ significantly, indicating the presence of fast and slow relaxation stages. The fast relaxation dominates at the initial stage of charging and discharging and is governed by interfacial processes, whereas the slow component is related to bulk diffusion and space-charge relaxation.

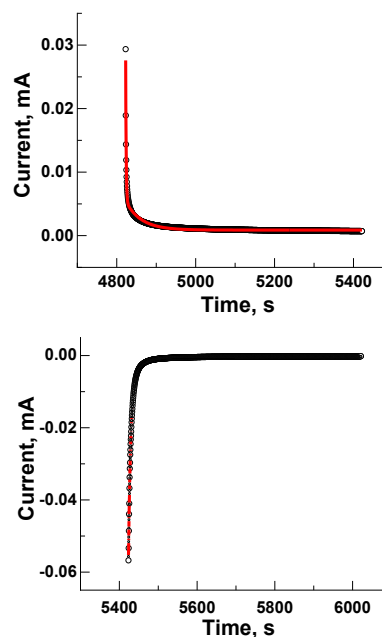


Fig. 3. Results of the approximation of the $I(t)$ dependences for the $\text{Ag}|\text{Ag}_{6.5}\text{P}_{0.5}\text{Ge}_{0.5}\text{S}_5\text{I}|\text{Se}$ composition during charging and discharging in the fifth cycle.

With increasing cycle number, the relaxation times become more stable, and the differences between neighboring cycles decrease. This behavior indicates gradual stabilization of the interfacial region and a reduction in the contribution of nonstationary processes.,

Current–Voltage Characteristics of $\text{Ag}|\text{Ag}_{7-x}(\text{Ge}_{1-x}\text{P}_x)\text{S}_5\text{I}|\text{Se}$ Heterostructures

The current–voltage characteristics of $\text{Ag}|\text{Ag}_{7-x}(\text{Ge}_{1-x}\text{P}_x)\text{S}_5\text{I}|\text{Se}$ heterostructures exhibit a pronounced nonlinear behavior and differ significantly from ohmic conduction. The CVCs demonstrate closed hysteresis loops, asymmetry with respect to zero voltage, and current maxima on both the anodic and cathodic branches (Fig. 5). These features indicate that the current in the cells is determined not only by the bulk ionic

conductivity of the superionic electrolyte but also by interfacial processes at the SE|Se interface, space-charge accumulation, and formation of an Ag₂Se-containing region (Fig. 1).

The Ag_{6.5}(Ge_{0.5}P_{0.5})S₅I composition exhibits the most pronounced nonstationary current response. This is consistent with the analysis of the I(t) dependences, where a two-stage relaxation behavior, the presence of fast and slow processes, and changes in relaxation parameters during cycling were observed for this composition. The relaxation times τ_1 and τ_2 differ significantly, indicating the separation of fast interfacial and slower diffusion-controlled processes. With increasing cycle number, the relaxation times tend to stabilize, reflecting the gradual “conditioning” of the heterostructure and the formation of a more stable interfacial state.

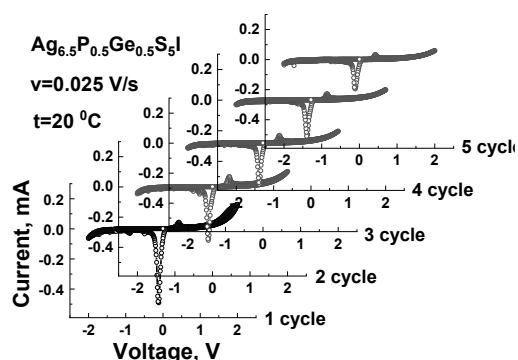


Fig. 5. Current–voltage characteristics of the Ag|Ag_{6.5}P_{0.5}Ge_{0.5}S₅I|Se cell during five consecutive cycles.

The asymmetry of the current–voltage characteristics with respect to zero voltage is associated with the difference between the processes occurring under positive and negative polarization. Under positive bias, Ag⁺ ions migrate from the silver electrode through the superionic electrolyte toward the selenium cathode. At the SE|Se interface, electrochemical interaction with selenium occurs, resulting in the formation of the Ag₂Se phase. Under reverse polarization, processes of partial decomposition or rearrangement of the Ag₂Se-containing region take place, along with reverse redistribution of Ag⁺ ions. Therefore, the forward and reverse voltage sweeps do not coincide, which manifests itself as hysteresis.

The presence of current maxima in the current–voltage characteristics is one of the key features of the investigated heterostructures. At the initial stage, the current increases with

increasing voltage due to enhanced Ag⁺ ion migration and activation of interfacial processes. After reaching the maximum, a further increase in voltage no longer leads to a proportional increase in current. This indicates a transition to a transport-limited regime in which the current is governed by space-charge accumulation, interface polarization, and the limited rate of the interfacial reaction at the SE|Se boundary. Similar features (nonlinearity, asymmetry, hysteresis, and current maxima) are characteristic of Ag|Ag_{7-x}(Ge_{1-x}P_x)S₅I|Se heterostructures and are associated with interfacial polarization and Ag₂Se formation.

An informative parameter is the hysteresis value ΔI at $U = 0$. A nonzero ΔI value indicates that even after passing through zero voltage, the system remains polarized. This means that an internal electric field associated with the accumulated space charge and the partially formed interfacial Ag₂Se region is preserved within the heterostructure. The larger the ΔI value, the more pronounced the nonequilibrium processes and the slower the charge relaxation.

With increasing cycle number, the parameters of the current–voltage characteristics change. In the initial cycles, more pronounced current maxima, a larger hysteresis loop area, and noticeable differences between the forward and reverse voltage sweeps are usually observed. This corresponds to the initial nonstationary state of the cell, during which efficient electrical contact is established, Ag⁺ ions are redistributed, and the SE|Se interfacial region is formed. In subsequent cycles, the shape of the current–voltage characteristics becomes more reproducible: the spread of current maxima decreases, the residual polarization value ΔI decreases, and the hysteresis loops become more stable. Such evolution indicates the transition of the heterostructure into a quasi-stationary state.

For the Ag_{6.5}P_{0.5}Ge_{0.5}S₅I composition, this cyclic evolution is of particular importance because the intermediate Ge/P ratio results in a complex energy landscape for Ag⁺ ion migration. On the one hand, structural disorder facilitates ionic transport; on the other hand, the presence of diffusion and interfacial limitations leads to pronounced polarization. Therefore, the current–voltage characteristics of this heterostructure reflect the competition between three processes: the fast ionic response of Ag⁺ ions to the external electric field, slower bulk diffusion in the

superionic ceramic, and the interfacial reaction associated with the formation/rearrangement of Ag_2Se .

The decrease in the current maximum on the reverse branch of the current–voltage characteristics with increasing cycle number in $\text{Ag}|\text{Ag}_{6.5}\text{P}_{0.5}\text{Ge}_{0.5}\text{S}_5\text{I}|\text{Se}$ heterostructures is associated with gradual stabilization of the SE|Se interfacial region and a reduction in the contribution of nonequilibrium processes. In the initial cycles, the electrochemical system is in a nonstationary state. During charging, intensive accumulation of Ag^+ ions occurs at the SE|Se interface together with the formation of an Ag_2Se -containing region. When the voltage sweep direction is reversed, a significant current maximum appears on the reverse branch due to the following processes: redistribution of the accumulated space charge; reverse migration of Ag^+ ions; partial decomposition or rearrangement of the interfacial Ag_2Se region; and strong interfacial polarization. In the initial cycles, the interfacial region has not yet been fully formed; therefore, the processes exhibit a pronounced nonequilibrium character. This results in large current maxima and broad hysteresis loops.

During subsequent cycling, the following processes occur:

1. Formation of a more stable Ag_2Se interfacial region.

The interfacial layer becomes more homogeneous and partially “adapted” to cyclic Ag^+ transport. As a result, the degree of structural rearrangement decreases during each subsequent cycle.

2. Reduction of space-charge accumulation.

After several cycles, the distribution of Ag^+ ions becomes more equilibrium-like, and the internal electric fields decrease. Therefore, a smaller amount of accumulated charge is released during the reverse voltage sweep.

3. Decrease in interfacial polarization.

As the SE|Se interface becomes stabilized, the contribution of polarization processes that generated additional current peaks in the initial cycles decreases.

4. Transition of the system to a quasi-stationary regime. The current–voltage characteristics become more reproducible, while the current peaks decrease. This corresponds to a reduced contribution of slow relaxation processes.

5. Partial irreversibility of interfacial processes.

A certain fraction of Ag_2Se may remain in the interfacial region even after discharge. Therefore,

in subsequent cycles the amplitude of reverse redistribution processes decreases, which also leads to a reduction of the current maximum on the reverse branch.

Physically, this means that the system gradually evolves from an “interface formation” regime to a regime of more stable ionic transport through an already formed interfacial region. Consequently, the current maximum on the reverse branch decreases together with the reduction of nonequilibrium processes and residual polarization.

Mechanical Properties of $\text{Ag}_{7-x}(\text{Ge}_{1-x}\text{P}_x)\text{S}_5\text{I}$ Superionic Ceramics Based on Nanoindentation Results.

The mechanical properties of $\text{Ag}_{7-x}(\text{Ge}_{1-x}\text{P}_x)\text{S}_5\text{I}$ superionic ceramic materials were investigated by micro- and nanoindentation methods. The mechanical response was analyzed using load–displacement (P – h) diagrams, which make it possible to determine hardness and elastic modulus (Fig. 6). For superionic materials, such investigations are important because the mechanical properties are closely related to the degree of structural disorder and the mobility of Ag^+ ions.

Typical P – h curves for $\text{Ag}_{7-x}(\text{Ge}_{1-x}\text{P}_x)\text{S}_5\text{I}$ ceramics are characterized by a smooth increase in indentation depth with increasing load, as well as by pronounced elastic–plastic deformation behavior. After unloading, partial recovery of the indentation depth is observed, indicating a significant elastic contribution to the overall deformation of the material. The Oliver–Pharr method was used to determine the mechanical parameters, according to which the hardness was calculated using the following relation [22]:

$$H = \frac{P_{\max}}{A}$$

where P_{\max} is the maximum applied load, and A is the contact area between the indenter and the sample surface. The effective elastic modulus was determined from the initial linear part of the unloading curve [22]:

$$E_r = \frac{\sqrt{\pi}}{2} \frac{S}{\sqrt{A}}$$

where S is the stiffness of the unloading branch of the P – h diagram.

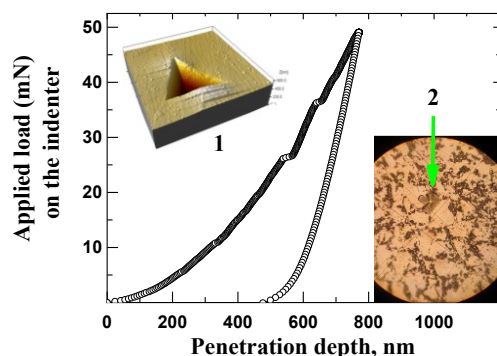


Fig. 6. Load–displacement curve for $\text{Ag}_{6.5}\text{Ge}_{0.5}\text{P}_{0.5}\text{S}_5\text{I}$ ceramic at room temperature. Imprints of the Knoop (1) and Vickers (2) indenters obtained during hardness measurements by micro- and nanoindentation.

The mechanical properties depend on the composition of $\text{Ag}_{7-x}(\text{Ge}_{1-x}\text{P}_x)\text{S}_5\text{I}$ and on the degree of heterovalent $\text{Ge} \leftrightarrow \text{P}$ substitution. With increasing phosphorus content, an increase in nanohardness and elastic modulus is observed, from $H=1.1$ GPa and $E=14.3$ GPa for $\text{Ag}_7\text{GeS}_5\text{I}$ to $H=2.1$ GPa and $E=27.3$ GPa for $\text{Ag}_6\text{PS}_5\text{I}$. Such changes in the mechanical properties are associated with modification of the superionic sublattice structure and variation in the degree of structural disorder. Substitution of Ge^{4+} by P^{5+} leads to changes in the distribution of Ag^+ ions, vacancy concentration, and the local energy landscape, which simultaneously affects both the transport and mechanical characteristics of the material.

Intercrystalline regions formed during recrystallization and sintering of ceramic materials play an important role in the formation of the mechanical properties of $\text{Ag}_{7-x}(\text{Ge}_{1-x}\text{P}_x)\text{S}_5\text{I}$ ceramics. Grain boundaries are structurally heterogeneous regions with an increased concentration of defects, local stresses, and micropores, which significantly affect the plastic deformation processes during indentation.

Intercrystalline boundaries can hinder deformation propagation and defect motion, resulting in an increase in hardness. A decrease in crystallite size increases the total area of grain boundaries, thereby enhancing the resistance to local plastic deformation.

For $\text{Ag}_{7-x}(\text{Ge}_{1-x}\text{P}_x)\text{S}_5\text{I}$ superionic ceramics, intercrystalline regions simultaneously represent zones of enhanced structural disorder and locally reduced packing density. In such regions, accumulation of micropores and defects formed

during recrystallization is possible, leading to a decrease in local mechanical rigidity. This effect is especially pronounced for compositions with increased Ge content, where an increase in crystallite size is accompanied by higher porosity and lower microhardness [23].

An additional factor is that intercrystalline regions in superionic materials may contain an increased concentration of mobile Ag^+ ions and structural vacancies. This promotes local relaxation of mechanical stresses under loading and facilitates plastic deformation of the material beneath the indenter. As a result, an increase in the degree of structural disorder in intergranular regions leads to a decrease in microhardness and elastic modulus.

Compositions with a higher degree of structural disorder are characterized by lower hardness values. This is associated with weakening of the local structural rigidity due to the increased dynamic mobility of the silver sublattice. In such materials, a more “soft” structure is formed, facilitating Ag^+ ion migration through a system of energetically close positions. Thus, a decrease in mechanical rigidity is accompanied by a certain increase in ionic mobility and a reduction in the energy barriers for ion transport.

For $\text{Ag}_{6.5}\text{Ge}_{0.5}\text{P}_{0.5}\text{S}_5\text{I}$ ceramics, intermediate values of hardness and Young’s modulus were observed ($H=1.4$ GPa, $E=18.2$ GPa). This composition exhibits the most pronounced two-stage relaxation behavior, separation of relaxation times τ_1 and τ_2 , and significant interfacial polarization. This indicates that, at the intermediate Ge/P ratio, an optimal balance between structural disorder and mechanical stability is achieved.

An important feature of nanoindentation in superionic ceramics is the possibility of observing local jumps in indentation depth (“pop-in” effects), which are associated with activation of local plastic deformation, defect motion, or structural rearrangement in the near-surface region. For $\text{Ag}_{7-x}(\text{Ge}_{1-x}\text{P}_x)\text{S}_5\text{I}$ materials, the presence of such features may be related to relaxation of internal stresses in regions with an increased degree of disorder. The appearance of “pop-in” effects indicates heterogeneity of the mechanical response and the complex nature of deformation processes in superionic ceramics. Thus, heterovalent $\text{Ge} \leftrightarrow \text{P}$ substitution makes it possible to control both the ionic

transport and mechanical characteristics of the material. The obtained results show that optimal functional properties are achieved through a balance between high Ag^+ ion mobility and sufficient mechanical stability of the ceramics, which is an important requirement for the application of such materials in solid-state electrochemical devices.

Conclusions

The ionic transport and mechanical properties of $\text{Ag}_{7-x}(\text{Ge}_{1-x}\text{P}_x)\text{S}_5\text{I}$ superionic ceramics and $\text{Ag}|\text{Ag}_{7-x}(\text{Ge}_{1-x}\text{P}_x)\text{S}_5\text{I}|\text{Se}$ heterostructures were investigated. It was established that the charge–discharge processes exhibit a relaxation character and can be described by a two-exponential model, indicating the presence of fast interfacial and slow diffusion-controlled processes. The current–voltage characteristics are characterized by nonlinearity, hysteresis, and current maxima caused by interfacial polarization and Ag_2Se formation at the SE|Se interface. It was shown that cycling leads to stabilization of the interfacial region and a reduction in the nonequilibrium character of charge transport processes. Nanoindentation results revealed that the decrease in microhardness and elastic modulus correlates with an increase in Ag^+ ion mobility. The obtained results indicate the existence of a relationship between the mechanical “softness” of the structure, the degree of disorder, and the efficiency of ionic transport in $\text{Ag}_{7-x}(\text{Ge}_{1-x}\text{P}_x)\text{S}_5\text{I}$ superionic ceramics.

This work has been supported by the grant of the Ministry of Education and Science of Ukraine under project No. 0126U002381. The authors express their gratitude to Senior Researcher A.I. Pogodin for providing samples of the superionic ceramics.

Conflict of Interest: The authors declare that there is no conflict of interest.

Authors' Contributions: Bilanych V.S.: conceptualization, methodology, validation, scientific supervision, results analysis, original writing; Slyvka A.A.: sample preparation, research, validation, data processing, participation in results analysis, original writing.

Reference

1. Alsaç E.P., Nelson D.L., Yoon S.G., Cavallaro K.A., Wang C., Sandoval S.E., Eze U.D., Jeong W.J., McDowell M. T. Characterizing electrode materials and interfaces in solid-state batteries. *Chemical Reviews*. 2025, 125(3). 2009–2119. Doi: 10.1021/Acs.Chemrev.4c00584.
2. Austin M.S., Galinat S.L., Maughan A.E. Complex dynamics in argyrodite solid-state ion conductors. *Chemistry of Materials*. 2026, 38(7). 3038–3058. Doi: 10.1021/acs.chemmater.5c02939.
3. Yamamoto O. Solid state ionics: A Japan perspective. *Science and Technology of Advanced Materials*. 2017, 18. 504–527. Doi: 10.1080/14686996.2017.1328955.
4. Wang H., Ozkan C.S., Zhu H., Li X. Advances in solid-state batteries: Materials, interfaces, characterizations, and devices. *MRS Bulletin*. 2023, 48. 1221–1229. Doi: 10.1557/s43577-023-00649-7.
5. Wang L., Li J., Lu G., Li W., Tao Q., Shi C., Jin H., Chen G., Wang S. Fundamentals of electrolytes for solid-state batteries: Challenges and perspectives. *Frontiers in Materials*. 2020, 7. 111. Doi: 10.3389/fmats.2020.00111.
6. Fong K.D., Self J., Diederichsen K.M., Wood B. M., McCloskey B.D., Persson K.A. Ion transport and the transference number. *ACS Central Science*. 2019, 5(7). 1250–1260. Doi: 10.1021/acscentsci.9b00406.
7. Nie K., Hong Y., Qiu J., Q. Li, X. Yu, H. Li, Li. Chen. Interfaces between cathode and electrolyte in solid-state batteries: Challenges and perspectives. *Frontiers in Chemistry*. 2018, 6. 1–19. Doi: 10.3389/fchem.2018.00616.
8. Studenyak I.P., Pogodin A.I., Filep M.J., Symkanych O.I., Babuka T.Y., Kokhan O.P., Kúš P. Influence of heterovalent cationic substitution on electrical properties of $\text{Ag}_{6+x}(\text{P}_{1-x}\text{Ge}_x)\text{S}_5\text{I}$ solid solutions. *Journal of Alloys and Compounds*. 2021, 873. 159784. Doi: 10.1016/j.jallcom.2021.159784.
9. Pogodin A.I., Filep M.J., Malakhovska T.O., Vakulchak V.V., Komanicky V., Izai V.Yu., Studenyak Y.I., Zhukova Y.P., Shender I.O., Bilanych V.S., Kokhan O.P., Kúš P. Microstructural, mechanical and electrical properties of superionic $\text{Ag}_{6+x}(\text{P}_{1-x}\text{Ge}_x)\text{S}_5\text{I}$ ceramic materials. *Journal of Physics and Chemistry of Solids*. 2022, 171. 111042. Doi: 10.1016/j.jpcs.2022.111042.
10. Pogodin A.I., Filep M.J., Malakhovska T.O., Vakulchak V.V., Komanicky V., Vorobiov S., Izai V. Yu., Satrapinskyy L., Shender I.O., Bilanych V.S., Kokhan O.P., Kúš P. Recrystallization and heterovalent substitution effects on mechanical and electrical parameters of $\text{Ag}_{6+x}(\text{P}_{1-x}\text{Ge}_x)\text{S}_5\text{I}$ -based ceramics. *Journal of the European Ceramic Society*. 2023, 44(6). 4097–4110. Doi: 10.1016/j.jeurceramsoc.2023.12.093.

11. Pogodin A.I., Filep M.J., Malakhovska T.O., Vakulchak V.V., Komanicky V., Vorobiov S., Izai V. Yu., Satrapinsky L., Shender I.O., Bilanych V.S., Kokhan O.P., Kúš P. Influence of recrystallization process on ionic conductivity of $\text{Ag}_{6.75}\text{P}_{0.25}\text{Ge}_{0.75}\text{S}_5\text{I}$ based ceramic materials. *Ceramics International*. 2023, 49(21). 33764–33772. Doi: 10.1016/j.ceramint.2023.08.068.
12. Bilanych V.S., Skubenykh K.V., Babilya M.I., Pogodin A.I., Studenyak I.P. The effect of isovalent cation substitution on mechanical properties of $(\text{Cu}_x\text{Ag}_{1-x})_7\text{SiS}_5\text{I}$ superionic mixed single crystals. *Ukrainian Journal of Physics*. 2020. 65(5), P.453–457. Doi: 10.15407/ujpe65.5.453.
13. Bilanych V.S., Slyvka A.A., Vorobiov S.I., Pogodin A.I., Malakhovska T.O., Mohylyuk I.M., Komanicky V. Charge-discharge processes in solid electrolyte heterostructures $\text{Ag}_{7-x}(\text{Ge}_{1-x}\text{P}_x)\text{S}_5\text{I}$ for electrochemical energy devices. *Semiconductor Physics, Quantum Electronics & Optoelectronics*. 2026, 29(1). 66–79. Doi: 10.15407/spqeo29.01.066.
14. Jindal S., Singh S., Saini G. S. S., Tripathi S.K. Optimization of thermoelectric power factor of (013)-oriented Ag_2Se films via thermal annealing. *Materials Research Bulletin*. 2021, 145. 111525. Doi: 10.1016/j.materresbull.2021.111525.
15. Cao T., Shi X.-L., Hu B., Yang Q., Lyu W.-Y., Sun S., Yin L.-C., Liu Q.-Y., Chen W., Wang X., Liu S., Li M., Liu W.-D., Tesfamichael T., Liu Q., MacLeod J., Chen Z.-G. Advancing Ag_2Se thin-film thermoelectrics via selenization-driven anisotropy control. *Nature Communications*. 2025, 16. 1555. Doi: 10.1038/s41467-025-56671-7.
16. Bilanych V.V., Csach K., Flachbart K., Bilanych V.S., Rizak V.M. Investigation of the processes of softening and crystallization of glassy selenium by dynamic mechanical analysis method. *Scientific Herald of Uzhhorod University. Series Physics*. 2018, 44. 44–51. Doi: 10.24144/2415-8038.2018.44.44-50.
17. Bilanych V.S., Slyvka A.A., Vorobiov S.I., Pogodin A.I., Malakhovska T.O., Mohylyuk I.M., Komanicky V. Charge-discharge processes in solid electrolyte heterostructures $\text{Ag}_{7-x}(\text{Ge}_{1-x}\text{P}_x)\text{S}_5\text{I}$ for electrochemical energy devices. *Semiconductor Physics, Quantum Electronics & Optoelectronics*. 2026, 29(1). 66–79. Doi: 10.15407/spqeo29.01.066.
18. Bard A.J., Faulkner L.R., White H.S. *Electrochemical Methods: Fundamentals and Applications* (3rd ed.). 2022, John Wiley & Sons.
19. Zhang Z., Shao Y., Lotsch B., Hu Y.-S., Li H., Janek J., Nazar L.F., Nan C.-W., Maier J., Armand M., Chen L. New horizons for inorganic solid state ion conductors. *Energy & Environmental Science*. 2018, 11(8). 1945–1976. Doi: 10.1039/C8EE01053F.
20. Banerjee A., Wang X., Fang C., Wu E.A., Meng Y.S. Interfaces and interphases in all-solid-state batteries with inorganic solid electrolytes. *Chemical Reviews*. 2020, 120(14). 6878–6933. Doi: 10.1021/acs.chemrev.0c00101.
21. Oliver W. C., Pharr G. M. An improved technique for determining hardness and elastic modulus using load and displacement sensing indentation experiments. *Journal of Materials Research*. 1992, 7(6). 1564–1583. Doi: 10.1557/JMR.1992.1564.
22. Kogai V.Y. Reaction-diffusion-induced explosive crystallization in a metal–selenium nanometer film structure. *Technical Physics*. 2016, 61 (3). 461–463. Doi: 10.1134/S1063784216030117.
23. Pogodin A.I., Filep M.J., Malakhovska T.O., Vakulchak V.V., Komanicky V., Vorobiov S., Izai V. Yu., Satrapinsky L., Shender I.O., Bilanych V.S., Kokhan O.P., Kúš P. Recrystallization and heterovalent substitution effects on mechanical and electrical parameters of $\text{Ag}_{6+x}(\text{P}_{1-x}\text{Ge}_x)\text{S}_5\text{I}$ -based ceramics. *Journal of the European Ceramic Society*. 2024, 44(6). 4097–4110, Doi: 10.1016/j.jeurceramsoc.2023.12.093.

Стаття надійшла до редакції: 30.04.2026 р.; прийнята до друку 18.05.2026 р.; опублікована 29.05.2026 р.

ІОННИЙ ТРАНСПОРТ ТА МЕХАНІЧНІ ВЛАСТИВОСТІ СУПЕРІОННОЇ КЕРАМІКИ $\text{Ag}_{7-x}(\text{Ge}_{1-x}\text{P}_x)\text{S}_5\text{I}$

Сливка А.А., Біланич В.С.

ДВНЗ «Ужгородський національний університет», 88000,
м. Ужгород, вул. Підгірна 46
e-mail: vitaliy.bilanych@uzhnu.edu.ua

Досліджено іонно-транспортні та механічні властивості суперіонних керамік $\text{Ag}_{7-x}(\text{Ge}_{1-x}\text{P}_x)\text{S}_5\text{I}$ та гетероструктур $\text{Ag}|\text{Ag}_{7-x}(\text{Ge}_{1-x}\text{P}_x)\text{S}_5\text{I}|\text{Se}$. Процеси заряджання-розряджання вивчали

методом циклічної потенціостатичної хроноамперометрії, а вольт-амперні характеристики - методом циклічної вольтамперометрії. Встановлено, що залежності $I(t)$ мають виражений релаксаційний характер та добре описуються двоекспоненціальною моделлю, що свідчить про наявність швидких міжфазних і повільних дифузійних процесів. Вольт-амперні характеристики характеризуються нелінійністю, гістерезисом і максимумами струму, зумовленими міжфазною поляризацією, накопиченням просторового заряду та формуванням шару Ag_2Se на межі SE|Se . Показано, що циклування приводить до стабілізації міжфазної області та зменшення внеску нерівноважних процесів. Методом наноіндентування встановлено кореляцію між твердістю, модулем пружності та ступенем структурного розупорядкування і рухливістю Ag^+ -іонів. Зменшення механічної жорсткості корелює з підвищенням ефективності іонного транспорту, що свідчить про важливу роль структурної «м'якості» у формуванні суперіонної провідності.

Ключові слова: суперіонні кераміки, іонний транспорт, $\text{Ag}_{7-x}(\text{Ge}_{1-x}\text{P}_x)\text{S}_5\text{I}$, зарядно-розрядні процеси, циклічна вольтамперометрія, хроноамперометрія, наноіндентування, структурне розупорядкування, твердотільні електроліти.

Список використаних джерел

1. Alsaç E.P., Nelson D.L., Yoon S.G., Cavallaro K.A., Wang C., Sandoval S.E., Eze U.D., Jeong W.J., McDowell M. T. Characterizing electrode materials and interfaces in solid-state batteries. *Chemical Reviews*. 2025, 125(3). 2009–2119. Doi: 10.1021/ Acs.Chemrev.4c00584.
2. Austin M.S., Galinat S.L., Maughan A.E. Complex dynamics in argyrodite solid-state ion conductors. *Chemistry of Materials*. 2026, 38(7). 3038–3058. Doi: 10.1021/acs. chemmater.5c02939.
3. Yamamoto O. Solid state ionics: A Japan perspective. *Science and Technology of Advanced Materials*. 2017, 18. 504–527. Doi: 10.1080/14686996.2017.1328955.
4. Wang H., Ozkan C.S., Zhu H., Li X. Advances in solid-state batteries: Materials, interfaces, characterizations, and devices. *MRS Bulletin*. 2023, 48. 1221–1229. Doi: 10.1557/ s43577-023-00649-7.
5. Wang L., Li J., Lu G., Li W., Tao Q., Shi C., Jin H., Chen G., Wang S. Fundamentals of electrolytes for solid-state batteries: Challenges and perspectives. *Frontiers in Materials*. 2020, 7. 111. Doi: 10.3389/fmats.2020.00111.
6. Fong K.D., Self J., Diederichsen K.M., Wood B. M., McCloskey B.D., Persson K.A. Ion transport and the transference number. *ACS Central Science*. 2019, 5(7). 1250–1260. Doi: 10.1021/acscentsci. 9b00406.
7. Nie K., Hong Y., Qiu J., Q. Li, X. Yu, H. Li, Li. Chen. Interfaces between cathode and electrolyte in solid-state batteries: Challenges and perspectives. *Frontiers in Chemistry*. 2018, 6. 1–19. Doi: 10.3389/fchem.2018.00616.
8. Studenyak I.P., Pogodin A.I., Filep M.J., Symkanych O.I., Babuka T.Y., Kokhan O.P., Kúš P. Influence of heterovalent cationic substitution on electrical properties of $\text{Ag}_{6+x}(\text{P}_{1-x}\text{Ge}_x)\text{S}_5\text{I}$ solid solutions. *Journal of Alloys and Compounds*. 2021, 873. 159784. Doi: 10.1016/ j.jallcom.2021.159784.
9. Pogodin A.I., Filep M.J., Malakhovska T.O., Vakulchak V.V., Komanicky V., Izai V.Yu., Studenyak Y.I., Zhukova Y.P., Shender I.O., Bilanych V.S., Kokhan O.P., Kúš P. Microstructural, mechanical and electrical properties of superionic $\text{Ag}_{6+x}(\text{P}_{1-x}\text{Ge}_x)\text{S}_5\text{I}$ ceramic materials. *Journal of Physics and Chemistry of Solids*. 2022, 171. 111042. Doi: 10.1016/j.jpcs.2022.111042.
10. Pogodin A.I., Filep M.J., Malakhovska T.O., Vakulchak V.V., Komanicky V., Vorobiov S., Izai V. Yu., Satrapinsky L., Shender I.O., Bilanych V.S., Kokhan O.P., Kúš P. Recrystallization and heterovalent substitution effects on mechanical and electrical parameters of $\text{Ag}_{6+x}(\text{P}_{1-x}\text{Ge}_x)\text{S}_5\text{I}$ -based ceramics. *Journal of the European Ceramic Society*. 2023, 44(6). 4097–4110. Doi: 10.1016/j. jeurceramsoc.2023.12.093.
11. Pogodin A.I., Filep M.J., Malakhovska T.O., Vakulchak V.V., Komanicky V., Vorobiov S., Izai V. Yu., Satrapinsky L., Shender I.O., Bilanych V.S., Kokhan O.P., Kúš P. Influence of recrystallization process on ionic conductivity of $\text{Ag}_{6.75}\text{P}_{0.25}\text{Ge}_{0.75}\text{S}_5\text{I}$ based ceramic materials. *Ceramics International*. 2023, 49(21). 33764–33772. Doi: 10.1016/j.ceramint.2023.08.068.
12. Bilanych V.S., Skubenych K.V., Babilya M.I., Pogodin A.I., Studenyak I.P. The effect of isovalent cation substitution on mechanical properties of $(\text{Cu}_x\text{Ag}_{1-x})_7\text{SiS}_5\text{I}$ superionic mixed single crystals. *Ukrainian Journal of Physics*. 2020. 65(5), P.453–457. Doi: 10.15407/ujpe65.5.453.
13. Bilanych V.S., Slyvka A.A., Vorobiov S.I., Pogodin A.I., Malakhovska T.O., Mohylyuk I.M., Komanicky V. Charge-discharge processes in solid electrolyte heterostructures $\text{Ag}_{7-x}(\text{Ge}_{1-x}\text{P}_x)\text{S}_5\text{I}$ for electrochemical energy devices. *Semiconductor Physics, Quantum Electronics & Optoelectronics*. 2026, 29(1). 66–79. Doi: 10.15407/ spqeo29.01.066.

14. Jindal S., Singh S., Saini G. S. S., Tripathi S.K. Optimization of thermoelectric power factor of (013)-oriented Ag_2Se films via thermal annealing. *Materials Research Bulletin*. 2021, 145. 111525. Doi: 10.1016/j.materresbull.2021.111525.
15. Cao T., Shi X.-L., Hu B., Yang Q., Lyu W.-Y., Sun S., Yin L.-C., Liu Q.-Y., Chen W., Wang X., Liu S., Li M., Liu W.-D., Tesfamichael T., Liu Q., MacLeod J., Chen Z.-G. Advancing Ag_2Se thin-film thermoelectrics via selenization-driven anisotropy control. *Nature Communications*. 2025, 16. 1555. Doi: 10.1038/s41467-025-56671-7.
16. Bilanych V.V., Csach K., Flachbart K., Bilanych V.S., Rizak V.M. Investigation of the processes of softening and crystallization of glassy selenium by dynamic mechanical analysis method. *Scientific Herald of Uzhhorod University. Series Physics*. 2018, 44. 44–51. Doi: 10.24144/2415-8038.2018.44.44-50.
17. Bilanych V.S., Slyvka A.A., Vorobiov S.I., Pogodin A.I., Malakhovska T.O., Mohylyuk I.M., Komanicky V. Charge-discharge processes in solid electrolyte heterostructures $\text{Ag}_{7-x}(\text{Ge}_{1-x}\text{P}_x)\text{S}_5\text{I}$ for electrochemical energy devices. *Semiconductor Physics, Quantum Electronics & Optoelectronics*. 2026, 29(1). 66–79. Doi: 10.15407/spqeo29.01.066.
18. Bard A.J., Faulkner L.R., White H.S. *Electrochemical Methods: Fundamentals and Applications* (3rd ed.). 2022, John Wiley & Sons.
19. Zhang Z., Shao Y., Lotsch B., Hu Y.-S., Li H., Janek J., Nazar L.F., Nan C.-W., Maier J., Armand M., Chen L. New horizons for inorganic solid state ion conductors. *Energy & Environmental Science*. 2018, 11(8). 1945–1976. Doi: 10.1039/C8EE01053F.
20. Banerjee A., Wang X., Fang C., Wu E.A., Meng Y.S. Interfaces and interphases in all-solid-state batteries with inorganic solid electrolytes. *Chemical Reviews*. 2020, 120(14). 6878–6933. Doi: 10.1021/acs.chemrev.0c00101.
21. Oliver W. C., Pharr G. M. An improved technique for determining hardness and elastic modulus using load and displacement sensing indentation experiments. *Journal of Materials Research*. 1992, 7(6). 1564–1583. Doi: 10.1557/JMR.1992.1564.
22. Kogai V.Y. Reaction-diffusion-induced explosive crystallization in a metal–selenium nanometer film structure. *Technical Physics*. 2016, 61 (3). 461–463. Doi: 10.1134/S1063784216030117.
23. Pogodin A.I., Filep M.J., Malakhovska T.O., Vakulchak V.V., Komanicky V., Vorobiov S., Izai V. Yu., Satrapinsky L., Shender I.O., Bilanych V.S., Kokhan O.P., Kúš P. Recrystallization and heterovalent substitution effects on mechanical and electrical parameters of $\text{Ag}_{6+x}(\text{P}_{1-x}\text{Ge}_x)\text{S}_5\text{I}$ -based ceramics. *Journal of the European Ceramic Society*. 2024, 44(6). 4097–4110, Doi: 10.1016/j.jeurceramsoc.2023.12.093.